Leukemia
https://doi.org/10.1038/s41375-020-0919-5

ARTICLE

Lymphoma

Frequent mutations in the amino-terminal domain of BCL7A impair its tumor suppressor role in DLBCL

Carlos Baliñas-Gavira[1,2,3] · María I. Rodríguez[1,2,4] · Alvaro Andrades[1,2] · Marta Cuadros[1,4,5] · Juan Carlos Álvarez-Pérez[1,2] · Ángel F. Álvarez-Prado[6] · Virginia G. de Yébenes[6,7] · Sabina Sánchez-Hernández[8] · Elvira Fernández-Vigo[9] · Javier Muñoz[9] · Francisco Martín[8] · Almudena R. Ramiro[6] · José A. Martínez-Climent[10] · Pedro P. Medina[1,2,4]

Received: 2 October 2019 / Revised: 6 June 2020 / Accepted: 9 June 2020

Abstract

Mutations in genes encoding subunits of the SWI/SNF chromatin remodeling complex are frequently found in different human cancers. While the tumor suppressor function of this complex is widely established in solid tumors, its role in hematologic malignancies is largely unknown. Recurrent point mutations in *BCL7A* gene, encoding a subunit of the SWI/SNF complex, have been reported in diffuse large B-cell lymphoma (DLBCL), but their functional impact remains to be elucidated. Here we show that BCL7A often undergoes biallelic inactivation, including a previously unnoticed mutational hotspot in the splice donor site of intron one. The splice site mutations render a truncated BCL7A protein, lacking a portion of the amino-terminal domain. Moreover, restoration of wild-type BCL7A expression elicits a tumor suppressor-like phenotype in vitro and in vivo. In contrast, splice site mutations block the tumor suppressor function of BCL7A by preventing its binding to the SWI/SNF complex. We also show that BCL7A restoration induces transcriptomic changes in genes involved in B-cell activation. In addition, we report that SWI/SNF complex subunits harbor mutations in more than half of patients with germinal center B-cell (GCB)-DLBCL. Overall, this work demonstrates the tumor suppressor function of BCL7A in DLBCL, and highlights that the SWI/SNF complex plays a relevant role in DLBCL pathogenesis.

Introduction

Diffuse large B-cell lymphoma (DLBCL) is the most common lymphoma, with an annual incidence of over 100,000 cases worldwide. Although most DLBCL patients achieve complete remission with frontline R-CHOP immunochemotherapy,

Supplementary information The online version of this article (https://doi.org/10.1038/s41375-020-0919-5) contains supplementary material, which is available to authorized users.

✉ Pedro P. Medina
pedromedina@ugr.es

1 Gene Expression Regulation and Cancer Group (CTS-993). GENYO. Centre for Genomics and Oncological Research: Pfizer-University of Granada-Andalusian Regional Government, Granada, Spain

2 Department of Biochemistry and Molecular Biology I, University of Granada, Granada, Spain

3 FIBAO - Fundación Pública para la Investigación Biosanitaria de Andalucía Oriental - Alejandro Otero, Granada, Spain

4 Instituto de Investigación Biosanitaria de Granada (ibis. GRANADA), Granada, Spain

5 Department of Biochemistry and Molecular Biology III and Immunology, University of Granada, Granada, Spain

6 B Cell Biology Lab, Centro Nacional de Investigaciones Cardiovasculares (CNIC), Madrid, Spain

7 Department of Immunology, Ophthalmology and ENT, School of Medicine, Complutense University, 12 de Octubre Health Research Institute (imas12), Madrid, Spain

8 Genomic Medicine Department, GENYO, Centre for Genomics and Oncological Research, Pfizer-University of Granada-Andalusian Regional Government, Granada, Spain

9 Proteomics Unit, CNIO—Spanish National Cancer Research Center, Madrid, Spain

10 Division of Haemato-Oncology, Centre for Applied Medical Research (CIMA), University of Navarra, CIBERONC, IDISNA, Pamplona, Spain

Published online: 24 June 2020

about 40% patients relapse and die of the disease [1]. Current limitations for effective treatment are related at least in part to the genetic heterogeneity of the tumors, which drives varied clinical presentations and therapeutic responses [2–5]. Gene expression analyses have provided further insights into the biological heterogeneity of DLBCL tumors by defining three major subgroups corresponding to the potential cells of origin: germinal center B-cell-like (GCB), activated B-cell-like (ABC) DLBCL, and primary mediastinal B-cell lymphoma [6, 7]. Risk stratification based on cell of origin classification holds prognostic significance and shows different therapeutic outcomes with current therapies [8, 9].

Next-generation sequencing (NGS) studies have revealed unique mutation patterns in GCB and ABC-DLBCL subgroups [5]. Mutations in gene components of the B-cell receptor and the NF-κB signaling pathways are predominantly found in the ABC subtype, whereas mutations involving chromatin modifiers are typically found in the GCB-DLBCL subtype, as well as in other germinal center (GC)-derived lymphomas including follicular lymphoma (FL) [10]. Among these epigenetic agents, the SWI/SNF chromatin remodeling complex is one of the most frequently altered in tumors [11]. This complex uses the energy released upon hydrolysis of ATP to alter the interactions between DNA and histones [12]. This process modifies the accessibility of DNA for the transcription machinery, altering gene expression [13]. Importantly, gene components of the SWI/SNF complex are frequently mutated in solid tumors [14, 15] as well as in hematologic malignancies [16], with an overall mutation rate of 20% across all cancers [17]. It has been widely established that the SWI/SNF complex has a tumor suppressor role in different solid tumors [11, 18–21]. However, despite their high prevalence, the functional role of SWI/SNF mutations in hematological malignancies including DLBCL is poorly understood.

The SWI/SNF complex was first discovered in yeast [22], where it has been extensively studied. However, new subunits, not found in yeast, have been recently identified as stable subunits in mammalian SWI/SNF complexes [17, 23]. These subunits include the BCL7A protein, whose specific biological role is largely unknown. BCL7A protein is highly expressed in the nuclei of GC B lymphocytes, but not in mature plasma cells [24]. Mutations in the *BCL7A* gene are recurrently found in DLBCL [25, 26] and in FL [27], but whether *BCL7A* mutations play a role in the pathogenesis of these GC-derived lymphomas remains to be determined.

Here we show that BCL7A often undergoes biallelic inactivation in DLBCL, including a previously unnoticed mutational hotspot in the splice donor site of intron one. We further show that BCL7A has tumor suppressor activity in DLBCL cells in vivo and in vitro, which is lost by splice site mutations that impede its binding to the SWI/SNF complex. Gene ontology (GO) enrichment analysis upon wild-type BCL7A restoration indicate that BCL7A plays a role on B-cell activation processes, and some of the altered genes, including *CDNK1A*, *TP63,* or *TRIB2* could explain the observed tumor suppressor phenotype.

Materials and methods

BCL7A mutation analysis

BCL7A was sequenced at the genomic DNA level in 41 DLBCL cell lines and 38 DLBCL primary tumors with the approval of Consejo Superior de Investigaciones Científicas, University of Salamanca, and University of Navarra Institutional Research Ethics Committees. Sets of primers were designed to amplify the coding region of BCL7A, including all splice sites. PCR products were analyzed by Sanger sequencing. Furthermore, whole-exome sequencing (WES) data from external datasets comprising a total of 1575 DLBCL patients were reanalyzed to include splice site mutations. See supplementary methods for additional information regarding human samples, cell lines, and the external datasets reanalyzed in this study.

In vivo bioluminescence imaging of murine xenograft

Δ27-BCL7A-expressing OCI-LY1 cell line expressing luciferase and transduced with BCL7A variants was intravenously tail vein injected in NSG mice ($n = 10$ mice/group). All animal care and procedures were performed in strict accordance with the recommendations in the Guide for the Care and Use of Laboratory Animals of the Bioethical Committee of the University of Granada and the study was approved by the Committee on the Ethics of Animal Experiments at the University of Granada. See Supplementary Methods for detailed information.

Competition cell growth assays and RNA-seq analysis

Δ27-BCL7A-expressing cell lines were transduced with lentiviral vectors expressing BCL7A variants and the fluorochrome ZsGreen1. The rate at which the percentage of Zsgreen1 declined over time was used to infer the relative growth disadvantage conferred by the transgene expression relative to the uninfected cells in the same culture. The percentage of ZsGreen1$^+$ cells was evaluated by FACS at different time points and normalized versus the percentage of ZsGreen1$^+$ cells at an initial time. Transduced cells were subjected to RNA-seq analysis. Libraries from mRNA were

prepared using 1 µg of RNA starting material and the TruSeq Stranded mRNA Library Prep Kit (Illumina). mRNA libraries were sequenced on the NextSeq 500 system (Illumina) using the highest output mode and paired-end 75 bp read lengths. See Supplementary Methods for detailed information.

Immunoprecipitation and LC–MS/MS analysis

Immunoprecipitates were digested with Lys-C/trypsin using the FASP protocol, and peptides were desalted with stage-tips. Samples were analyzed by LC–MS/MS on a Q Exactive Plus instrument coupled to an Ultimate 3000 nanoLC system. The mass spectrometer was operated in data-dependent mode and peptides were fragmented using higher-energy collisional dissociation. Protein identification and label-free quantification was done with MaxQuant using the standard settings. Statistical analysis was done with ProStar (v 1.12.12) using Limma, and FDR was estimated using the Benjamini–Hochberg method. Only proteins with a p value <0.05 and log2 ratio >3 were considered as potential interactors.

Statistical analyses

Unless specified otherwise, all statistical analyses were performed using R (version 3.6.1). Normality of continuous data was assessed using Q–Q plots and Shapiro–Wilk tests and the subsequent statistical tests were chosen accordingly.

Results

BCL7A splice site mutations represent a major hotspot in DLBCL samples

To study the potential impact of mutations in BCL7A function, we first screened for *BCL7A* mutations in a collection of 41 DLBCL cell lines. The *BCL7A* gene is located on chromosome 12q24.31 and its mature transcript is composed of six exons. *BCL7A* has two alternative isoforms that are co-expressed due to an extended exon variant located in the exon 5 (Fig. 1a). Missense mutations, mapping within the first exon, were found in the DB, OCI-LY7, ROS-50, and VAL cell lines at amino acid positions 8, 11, and 29, while the OCI-LY1 cell line exhibited a start-loss mutation (Supplementary Table 1). In addition, three different mutations in the splice donor site of intron 1 were found in Karpas-1106, OCI-LY1, and VAL cell lines (Fig. 1b and Supplementary Table 1). Further, the *BCL7A* gene was homozygously deleted in HBL1 cells, which was confirmed by a TaqMan copy number assay (Supplementary Fig. 1).

Detailed study of the mRNAs derived from splice site mutant *BCL7A* revealed that the splicing machinery uses a cryptic splice site donor sequence within the first exon (Fig. 1a and Supplementary Fig. 2a, b). As a consequence, the resulting mature mRNA is 81 nucleotides shorter (Fig. 1a and Supplementary Fig. 2c, d), but remains in-frame and the resultant protein loses 27 amino acids (S5_W31del) at the amino-terminal region (Δ27-BCL7A). In addition, along with the splice site mutations, OCI-LY1, Karpas-1106, and VAL cells harbor a second hit in the other allele. First, OCI-LY1 and VAL cell lines have mutations in the start codon and R11 respectively (Supplementary Fig. 3). Second, Karpas-1106 has a chromosomal rearrangement that creates a tandem duplication, characterized at the mRNA level, affecting exons 2 and 3 (Supplementary Fig. 4). These second hits observed in different alleles in cell lines harboring splice site mutations imply *BCL7A* biallelic loss, that results in the absence of wild-type BCL7A expression. Therefore, cell lines harboring splice site mutations only express a truncated Δ27-BCL7A, as was validated by western blot analyses (Supplementary Fig. 5).

To determine whether such findings in DLBCL cell lines were also observed in primary tumors, genomic DNA from 38 DLBCL patient samples was sequenced for the presence of *BCL7A* gene changes. Mutations were found in two samples (5.3%) (Fig. 1b and Supplementary Table 1). To extend our results to additional patient cohorts, we focused on the two largest DLBCL WES datasets from Reddy et al. [25] (1001 DLBCL patients) and from Schmitz et al. [26] (574 DLBCL patients). However, we realized that the analyses performed in the original articles were not suited to study BCL7A splice site mutations, as Reddy et al. restricted their analysis to exonic mutations, and Schmitz et al. filtered out most BCL7A splice site mutations by heuristic filtering criteria. Reanalysis of both datasets allowed the discovery of 28 and 7 BCL7A splice site mutations in patients from Reddy et al. and Schmitz et al., respectively (Fig. 1c and Supplementary Table 2). In addition, detailed inspection in Integrative Genomics Viewer suggested a potential overfiltering of start-loss and R11 mutations in *BCL7A* in the dataset from Reddy et al. [25] (Supplementary Table 2). To determine whether these mutations were somatic, we noted that mutations in the start codon or R11 in *BCL7A* are not found in cohorts of over 100,000 subjects without cancer from gnomAD (https://gnomad.broadinstitute.org), and that heterozygous mutations in the first splice site of *BCL7A* are present in gnomAD at allele frequencies below $1/10^5$ ($N =$ 145,172 sequenced alleles at c.92 + 1). Further, we found external evidence of somatic mutations at c.92 + 1 of *BCL7A* in three COSMIC B-cell lymphoma samples and one TCGA-DLBC sample (Supplementary Table 3). In addition, the two c.92 + 2 mutations in the data from

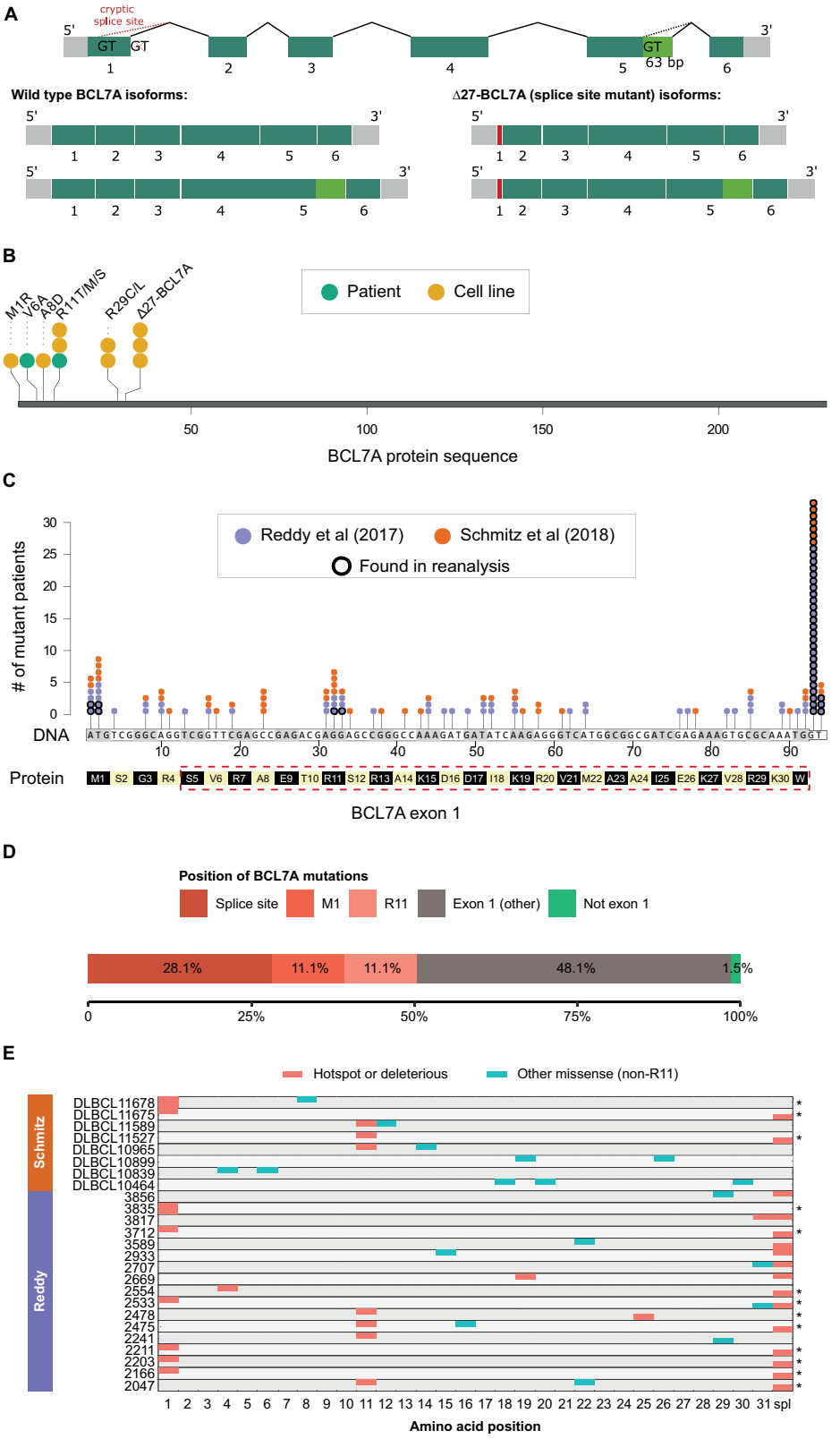

Fig. 1 Mutational patterns in BCL7A in DLBCL samples. **a** Structure of the *BCL7A* gene. Exons are colored in green and untranslated regions are colored in gray. The differential region in exon 5 between the short and long isoforms is highlighted in light green. **b** Lolliplot of BCL7A mutations at the protein level in a collection of 41 DLBCL cell lines and 38 DLBCL patients. Each circle represents one mutated sample. **c** Lolliplot of BCL7A mutations at the DNA level in exon 1 and first splice donor site in Reddy et al. [25] and in Schmitz et al. [26] cohorts. Outlined circles represent the novel mutations found in our reanalysis. Deleted amino acids in the Δ27-mutant BCL7A (S5_W31del) are outlined by a red dashed box. **d** Distribution of mutations in the *BCL7A* gene after combining the datasets from Reddy et al. [25] and Schmitz et al. [26]. The three significant mutational hotspots according to our analysis are shown in red. **e** BCL7A biallelic inactivation findings in DLBCL patients. Patient IDs from Schmitz and Reddy datasets are shown in the *y*-axis. For every patient, each allele is represented as an individual row and the different amino acids + splice donor site (spl) are depicted in the *x*-axis. Asterisks are shown at the right edge to indicate those patients that show a biallelic inactivation pattern, where there is a coexistence in different alleles of inactivating or R11 mutations (colored in red). Other missense mutations different from R11 mutations are colored in blue.

Schmitz et al. [26] were already confirmed to be somatic in the original study. Taken together, these facts indicate that despite the lack of germline information from most analyzed patients, our newly identified mutations in *BCL7A* are likely to be somatic. We will henceforth refer to splice donor site mutations, frameshift mutations, start-loss

mutations, or stop gain mutations in BCL7A together as "inactivating mutations", as supported by further evidence that will be discussed in the next sections.

BCL7A amino-terminal domain undergoes tumor suppressor-like inactivation in DLBCL

When we combined both external datasets, the inclusion of our newly identified mutations increased the mutation frequency of BCL7A by 30%, from 5.1% (80/1575) to 6.6% (104/1575) mutated patients. Most BCL7A mutations are located at the first exon or at the splice donor site of intron 1 (133/135). In addition, the mutations preferentially affected a highly significant mutational hotspot in the first splice donor ($p = 8.24 \times 10^{-25}$), as well as two less significant hotspots at R11 ($p = 1.20 \times 10^{-4}$) and at the start codon ($p = 1.20 \times 10^{-4}$) (Fig. 1d). Overall, inactivating mutations and missense mutations at the R11 hotspot were more than half (73/135) of all BCL7A mutations. We found 15 patients affected by more than one inactivating mutation and/or R11 mutation (Supplementary Table 4). In all of these cases but two, these mutations were present in different alleles (Fig. 1e). We did not observe allelic exclusion patterns with missense mutations other than R11 and M22L, but only two cases were affected by M22L mutations. The mutant allele frequencies were ≥30% in more than half (43/73) of the inactivating or R11 mutations and they were ≥70% for three of the splice site mutations, even without accounting for tumor purity or heterogeneity. High allele frequencies are characteristic of early drivers. Taken together, these results suggest that BCL7A recurrently undergoes biallelic loss in a significant fraction of cases, a typical feature of tumor suppressor genes.

Activation-induced deaminase (AID) targeting does not fully explain BCL7A mutational landscape

Previous studies have shown that *BCL7A* is an AID target [28] and that *BCL7A* mutations follow an AID signature in GC-derived lymphomas [29, 30]. In normal GC B cells, AID generates mutations in immunoglobulin genes at a high rate in a process known as somatic hypermutation (SHM) [31]. However, aberrant SHM can be identified in non-immunoglobulin gene loci, potentially generating mutations that contribute to genome instability and B-cell lymphomagenesis [32]. In this work, we have applied NGS to analyze AID-induced mutations in *Bcl7a* in GC B cells from mouse Peyer's Patches [33]. The frequency of transition mutations in cytosine/guanine (C/G) pairs in GC B cells from *Aicda* knockout mice, and from $Ung^{-/-}Msh2^{-/-}$ mice were compared. UNG and MSH2 back up each other to faithfully repair AID-induced lesions [34], but in the absence of UNG and MSH2, AID-induced deaminations remain unprocessed and lead to C → T and G → A transitions, the footprint of AID events [35, 36]. First, genomic DNA from GC B cells was used to amplify a 790 bp region and the PCR product was analyzed by NGS. Subsequent *Bcl7a* sequencing analysis was restricted to a 312 bp region that was covered by more than 100 high quality reads rather than the original 790 bp amplicon. The 312 bp region includes the *Bcl7a* 5′-UTR and the first exon (Fig. 2a). Then, we analyzed the C/G transition frequency within WRCY/RGYW sequences, which are the most highly mutated AID hotspots [37]. These sequences were highly mutated in *Bcl7a* in AID-proficient B cells in comparison with AID-deficient B cells (Fig. 2b). We next evaluated the correlation between *Bcl7a* mutations found in our mouse model and *BCL7A* mutations identified in DLBCL patients. Nucleotides with the highest net transition frequency in AID-proficient mice are usually mutated in human DLBCL samples (Fig. 2c). However, high transition frequency in our mouse model does not correlate with high *BCL7A* mutation prevalence in human DLBCL samples. On the one hand, start codon and R11 mutations do not overlap with AID hotspots and have null transition frequency in our mouse model. On the other hand, the RGYW motif in the first splice site is highly mutated in DLBCL patients but has relatively low transition frequency in our mouse model. Taken together, these observations suggest that AID targeting does not fully explain the BCL7A mutational pattern in DLBCL primary tumors. Our data also support that splice site mutations provide a growth advantage in tumoral cells since they are overrepresented compared with the wide spectrum of AID-induce mutations observed in non-transformed GC B cells.

The BCL7A amino-terminal domain is critical for its interaction with the SWI/SNF complex

The BCL7A amino-terminal domain (BCL7_Nt) harbors most BCL7A mutations, suggesting that BCL7_Nt is critical for the tumor suppressor phenotype. This BCL7_Nt domain is evolutionarily conserved and shared with the other two members of the BCL7 gene family: BCL7B and BCL7C [38]. Because BCL7A is a subunit of the SWI/SNF complex, we postulated that splice site mutations are positively selected in order to prevent BCL7A from binding to the SWI/SNF complex by removing the BCL7_Nt domain. To evaluate this hypothesis, we performed BCL7A immunoprecipitation studies in HBL1 cells completely lacking BCL7A expression (Supplementary Fig. 5b), which were transduced with wild-type BCL7A or mutant Δ27-BCL7A. Then, we analyzed whether SMARCA4, the catalytic subunit of the SWI/SNF complex, was pulled down with BCL7A. Whereas wild-type BCL7A bound to SMARCA4, Δ27-BCL7A did not (Fig. 3a). To further investigate the

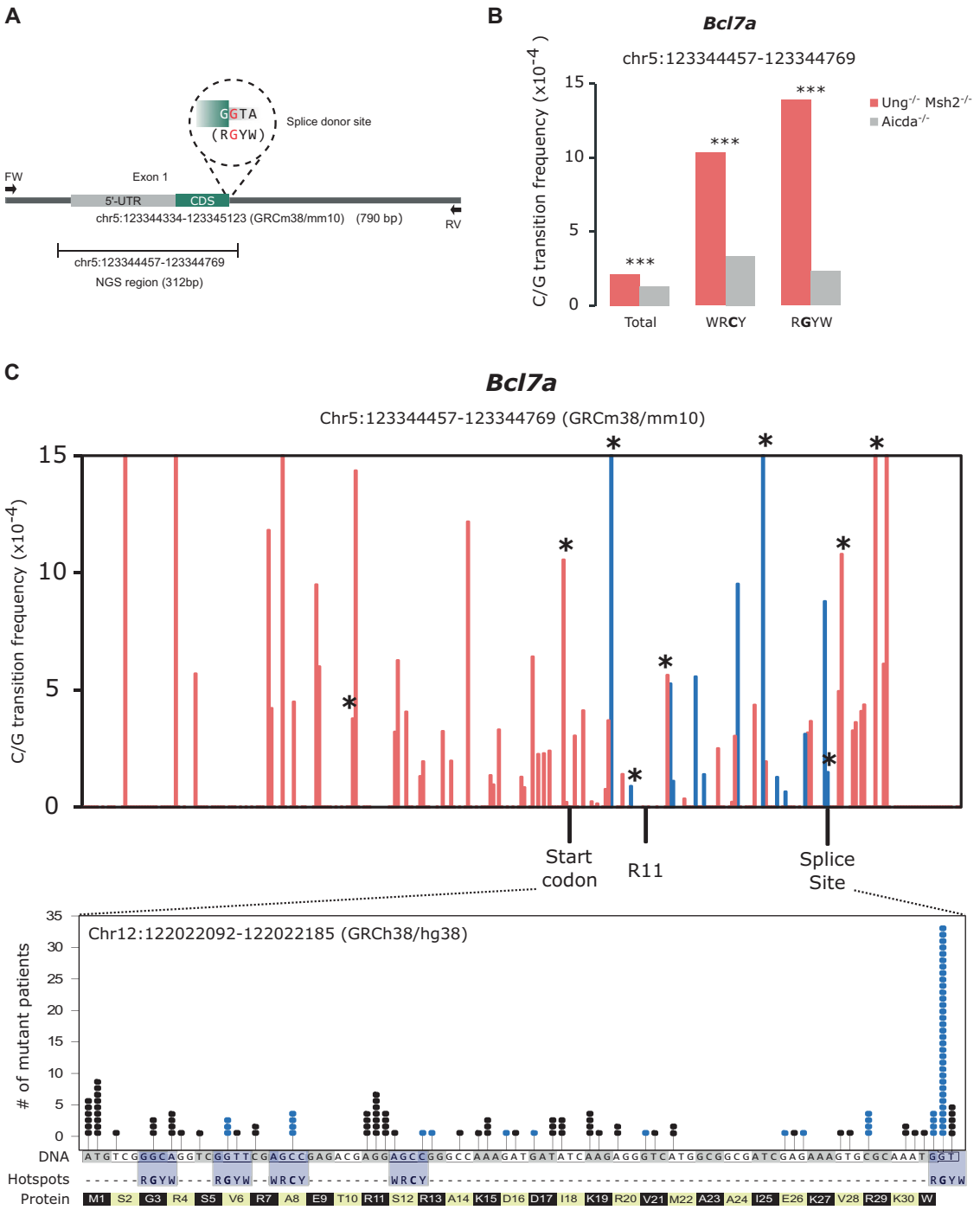

Fig. 2 BCL7A is targeted by AID. a A genomic region covering the 5′-UTR and the first exon of *Bcl7a* was PCR-amplified and subsequently sequenced by NGS. The genomic coordinates of the full amplicon (790 bp) and the region subjected to mutation analysis after quality filtering (312 bp, see Supplementary Methods) are indicated. **b** Transition frequency in total C/G nucleotides and in C/G within WRC(Y)/(R)GYW hotspots (W = A/T; R = G/A; Y = C/T) at the indicated *Bcl7a* locus in Ung$^{-/-}$Msh2$^{-/-}$ and Aicda$^{-/-}$ Peyer's Patches GC B cells. Two-tailed Fisher test; $^{***}p < 10^{-4}$. **c** Correlation between AID targeting in our mouse models and mutations in DLBCL patients. **Upper panel** Base per base analysis over the 312 bp amplicon whose genome coordinates are shown. The graphic shows the net transition frequency (TS_freq) in C/G (net TS_freq = TS_freq Ung/Msh2 dKO—TS_freq Aicda KO). Those nucleotide positions that correlate with mutations found in DLBCL samples have been colored in blue and asterisks have been placed in C/G nucleotides within WRCY/RGYW hotspots. Nucleotide positions relative to mutational hotspots (Start codon, R11, and splice site) in human DLBCL samples have been indicated in the bottom edge of the upper panel. **Lower panel** Lolliplot of BCL7A mutations at the DNA level in the region extending from the BCL7A start codon to the first splice donor site in Reddy et al. [25] and in Schmitz et al. [26] cohorts. Blue circles indicate those mutations that match with blue peaks from the upper panel. WRCY/RGYW hotspots, highlighted in blue, as well as the protein sequence are shown.

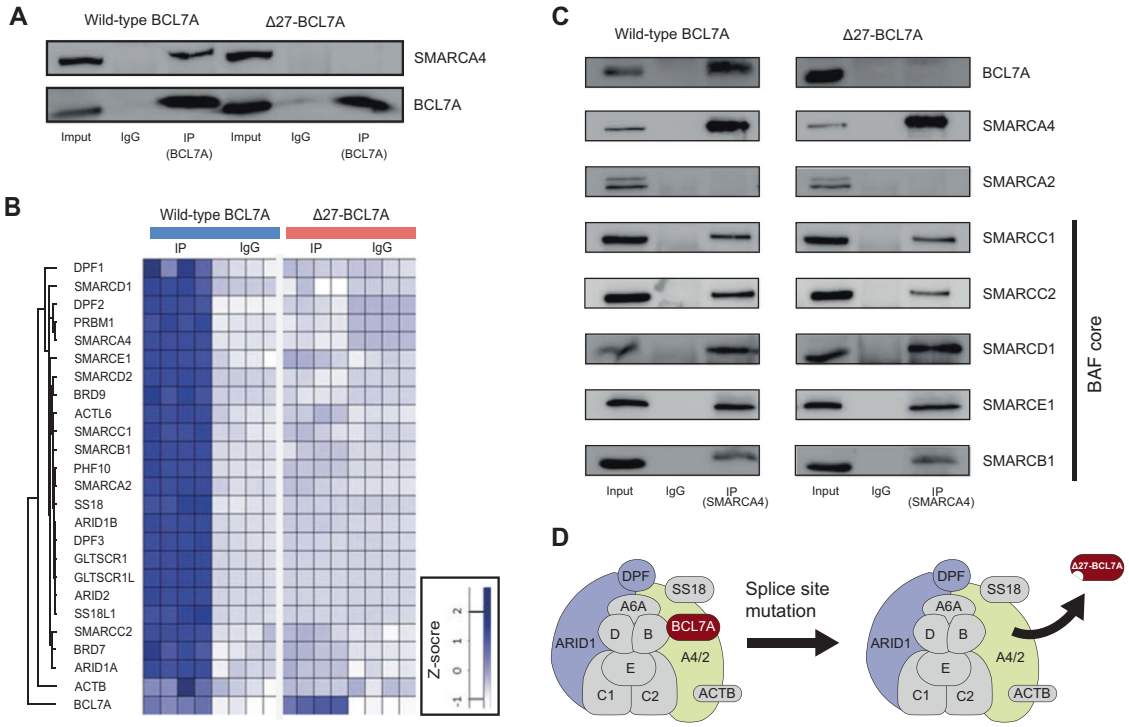

Fig. 3 Loss of BCL7A_Nt domain abolishes BCL7A binding to the SWI/SNF complex. a Immunoprecipitation of BCL7A using total protein extracts from HBL1 cells transduced with wild-type BCL7A or Δ27-BCL7A was performed. Co-immunoprecipitation of BCL7A and SMARCA4 subunits of the SWI/SNF complex was assessed by immunoblotting. Displayed gel is a representative image after performing the experiment twice. **b** Mass spectrometry analysis of mSWI/SNF complex subunits. BCL7A immunoprecipitation was used to purify complexes in HBL1 cells transduced with wild-type BCL7A or Δ27-BCL7A. Two biological replicates were performed for each condition (IP and IgG) and each replicate was run twice. Label-free quantification (LFQ) values are represented after *Z*-score normalization. All the subunits depicted in the heatmap were detected as a BCL7A interactors; $p < 0.05$ and log2FC > 3. DPF1 and ACTB were the only two subunits with a log2FC < 3 (1.4 and 1.8, respectively). **c** Immunoprecipitation of SMARCA4 immune complexes using total protein extracts from HBL1 cells transduced with wild-type BCL7A or Δ27-BCL7A. Co-immunoprecipitation of BCL7A, SMARCA4, SMARCA2, and BAF core subunits of the SWI/SNF complex was assessed by immunoblotting. **d** Schematic representation of BAF SWI/SNF residual complex. BCL7A is no longer able to bind to the SWI/SNF complex after BCL7A_Nt domain loss due to a splice site mutation. SWI/SNF complex subunits are abbreviated. Letters A4/2, B, C1, C2, D, and E represent the different "SMARC" subunits. A6A = ACTL6A; ARID1 = ARID1A/B; DPF = DPF1/2/3; SS18 = SS18 or SS18L1.

composition of the residual SWI/SNF complex and which subunits could remain attached to BCL7A or Δ27-BCL7A, we carried out liquid chromatography tandem mass spectrometry (LC–MS/MS). As expected, all SWI/SNF subunits were detected in the wild-type BCL7A pull-downs. However, none of the SWI/SNF subunits remained attached when Δ27-BCL7A was pulled down (Fig. 3b). We then asked whether BCL7A exclusion from the SWI/SNF complex modifies the interactions between SMARCA4 and core SWI/SNF complex subunits. BCL7A status did not affect the binding of SMARCA4 to core SWI/SNF complex subunits as they co-immunoprecipitated with SMARCA4 immune complexes in wild-type and Δ27-BCL7A-expressing cells (Fig. 3c). Altogether, these results show that the BCL7_Nt domain, which is lost due to splice site mutations, is necessary for BCL7A to bind to the SWI/SNF complex, but BCL7A absence does not affect the integrity of the residual complex (Fig. 3d).

BCL7A expression restoration has a tumor suppressor role in vitro and in vivo

Next, we assessed the functional role of *BCL7A* variants in B-cell lymphomagenesis. To evaluate the effect of restoring BCL7A expression, we focused on DLBCL cell lines that do not express wild-type BCL7A protein. To this end, we developed a growth competition assay in OCI-LY1 cells, which exclusively express Δ27-BCL7A, and VAL cells, which express truncated Δ27-BCL7A and mutant R11T BCL7A. We transduced both cell lines with different lentiviral constructions stably co-expressing BCL7A variants along with the fluorochrome ZsGreen1. In order to validate our models, BCL7A variants expression and protein levels were measured by RT-qPCR and western blot respectively (Supplementary Fig. 6a, b). Restoration of wild-type BCL7A resulted in growth impairment in OCI-LY1 and VAL cell lines in comparison with cells transduced with the

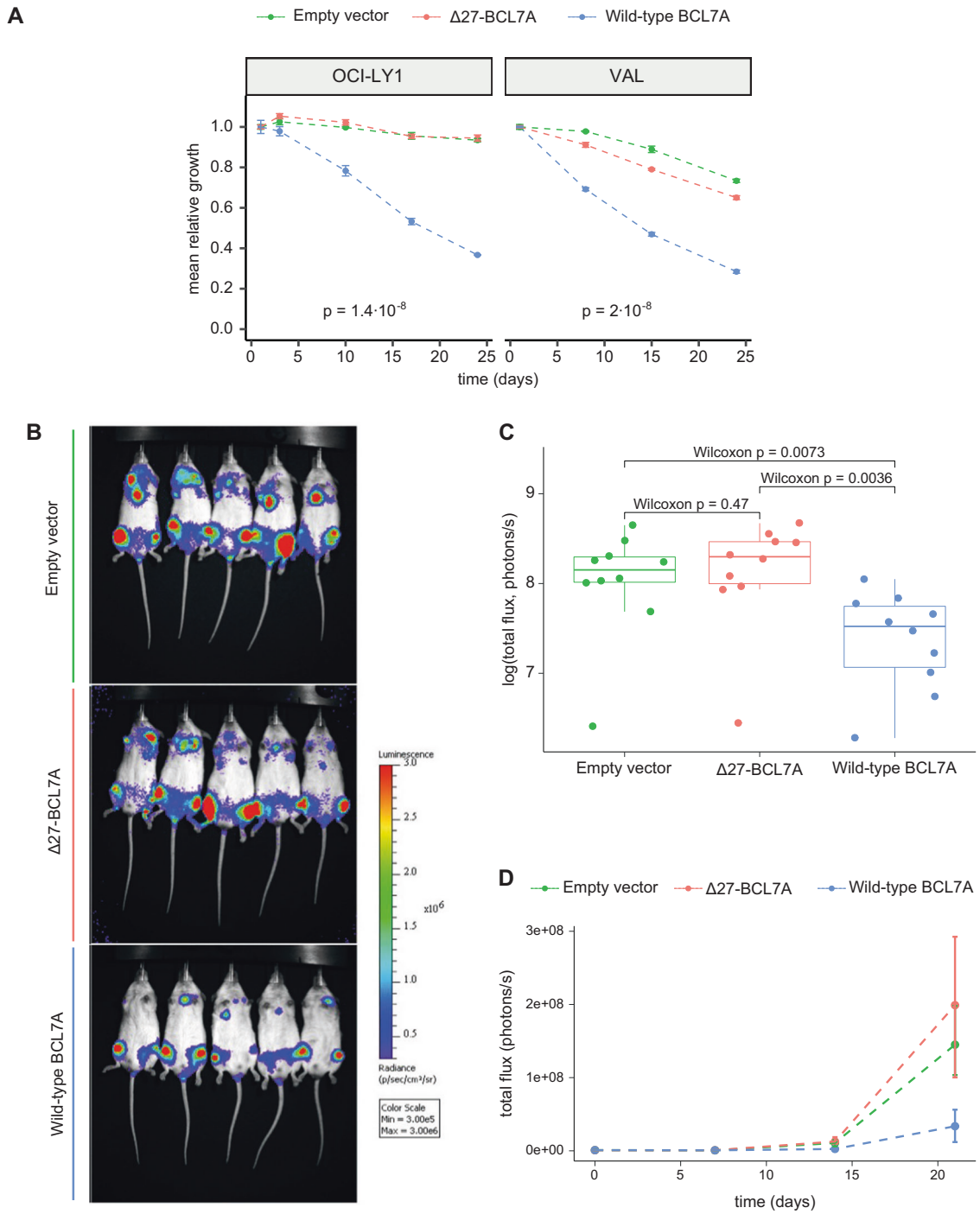

empty vector and with Δ27-BCL7A (Fig. 4a). Independent expression of short or long wild-type and Δ27-BCL7A induced equivalent growth impairment phenotype (Supplementary Fig. 6c). Of note, the phenotype induced by Δ27-BCL7A expression was not significantly different from the phenotype induced by the empty vector (end point *t*-test, $P > 0.05$). These data suggest that BCL7A plays a tumor suppressor role in DLBCL cells, which is lost by splice site mutant Δ27-BCL7A.

To further evaluate the tumor suppressor activity of BCL7A, we used in vivo image technologies (IVIS Spectrum) in the Δ27-BCL7A-expressing OCI-LY1 cell line. Stable OCI-LY1 cell lines expressing luciferase and transduced with BCL7A variants or empty vector were generated. Then, 5×10^6 cells were intravenously injected in three different cohorts of ten immunodeficient mice each, and monitored for in vivo luminescence for 3 weeks. The changes in bioluminescence over the time were different

◀ **Fig. 4 In vitro and in vivo analyses show that restoration of BCL7A drives a tumor suppressor-like phenotype. a** In vitro competitive growth assay in Δ27-BCL7A-expressing DLBCL cell lines transduced with either (i) empty vector, (ii) Δ27-BCL7A, or (iii) wild-type BCL7A. ZsGreen1$^+$ cells were sorted 5 days after transduction and cells were grown until obtaining ~5×10^6 total cells. Then, ZsGreen1$^+$ cells were mixed with sorted ZsGreen$^-$ cells to obtain three independent cultures per condition with 1×10^6 total cells per culture and an initial ~60% of ZsGreen1$^+$ cells. The mean %ZsGreen1$^+$ cells at each time point was normalized against the mean %ZsGreen1$^+$ cells at day 1. The start points (day 1) for competition cell growth analysis were 8 and 15 days after transduction for OCI-LY1 and VAL cell lines, respectively. The ANOVA p values for the comparisons at the end point of the experiment are shown. **b**, **c**, **d** Mice were injected with the Δ27-BCL7A-expressing OCI-LY1 cell line transduced with either (i) empty vector, (ii) Δ27-BCL7A, or (iii) wild-type BCL7A. Injected cells at day 0 (12 days after transduction with BCL7A constructs) were only reporter positive cells after sorting of ZsGreen1$^+$ cells. Ten mice per group were used. Mice were imaged at 0, 7, 14, and 21 days post injection using an IVIS spectrum imaging system. **b** Ventral pictures at day 21 of the top five mice with the highest bioluminescence signal per group. **c** Log-transformed bioluminescence signal at day 21 (10 mice per group in ventral position). Pairwise comparisons were performed using a Wilcoxon rank-sum test. **d** Quantification of the total photon flux in mice over the time (10 mice per group in ventral position). The error bars represent the interquartile range.

between the groups, so that log-luciferase expression at day 21 post injection was significantly lower in the wild-type BCL7A group in comparison with the Δ27-BCL7A and the empty vector groups (Fig. 4b–d). These results, together with data from the competitive cell growth assays, indicate the BCL7A plays a suppressor role in DLBCL, which is abolished by mutations in the splice donor site.

BCL7A is involved in B-cell activation

To gain further insights into the functional consequences of wild-type BCL7A expression restoration, we performed RNA sequencing in the OCI-LY1 and VAL cell lines under three conditions: wild-type BCL7A overexpression, Δ27-BCL7A overexpression and transduction with the empty vector. Two biological replicates were obtained for each condition. Differential expression analysis validated our model confirming that BCL7A was the top overexpressed gene when comparing wild-type BCL7A overexpression vs. the empty vector (fold change (FC) = 3.71 for OCI-LY1 and 1.61 for VAL), as well as for Δ27-BCL7A overexpression vs. empty vector (FC = 3.76 for OCI-LY1 and 1.70 for VAL), but not when comparing the overexpression of wild-type BCL7A vs. Δ27-BCL7A (FC = 0.99 for OCI-LY1 and 0.95 for VAL).

Focusing on the comparison between the wild-type BCL7A and Δ27-BCL7A expression models, we identified 320 differentially expressed genes in OCI-LY1 and 978 in VAL (adjusted p value <0.05) (Fig. 5a). Remarkably, 162 of the differentially expressed genes, more than half of the altered genes in OCI-LY1, were in common between both cell lines (Supplementary Fig. 7a). To determine whether these common altered genes group in any functional pathways, we performed a GO enrichment analysis using Metascape [39]. The top enriched pathways were related to B-cell biology (Fig. 5b) and include: regulation of B-cell activation, leukocyte cell-to-cell adhesion, cytokine mediated signaling pathway, and lymphocyte differentiation. Among them, "regulation of B-cell activation" (GO: 00508064) stands out with the highest significance ($p = 1.14 \times 10^{-11}$) and includes 31 genes that were differentially expressed in both VAL and OCI-LY1 cell lines (Supplementary Fig. 7b). Among these genes, CDNK1A (p21) expression is known to be regulated during B-cell differentiation, allowing a permissive proliferation state needed for B-cell clonal expansion [40, 41]. Western blot analysis showed that CDNK1A was upregulated upon wild-type BCL7A expression restoration (Supplementary Fig. 5c). Other genes related to proliferation that were differentially expressed after wild-type BCL7A expression restoration were TP63 or TRIB2 (Fig. 5c). On the one hand, the tumor suppressor gene TP63, which is known to modulate CDNK1A transcription [42], was upregulated in wild-type BCL7A-expressing cells. On the other hand, we found downregulation of TRIB2, which acts as an oncogene in hematological malignancies [43] and that has been recently found to promote tumorigenesis by blocking the AP4/CDKN1A signaling pathway [44]. Taken together, our results suggest that BCL7A modulates the expression of key B-cell genes that can be linked to a tumor suppressor phenotype.

Gene components of the SWI/SNF complex are commonly mutated in GCB-DLBCLs

We next determined whether, in addition to BCL7A, other members of the SWI/SNF complex showed genetic changes in DLBCL. For this purpose, we reanalyzed the cohorts used by Reddy et al. [25] and Schmitz et al. [26]. We considered all known members of human BAF, pBAF, and ncBAF SWI/SNF complexes, a total of 31 [45, 46], and we included the newly found *BCL7A* mutations in our analysis. A total of 290 of 1001 patients (29%) from Reddy et al. and 238 of 574 patients (41.5%) from Schmitz et al. showed mutations in at least one SWI/SNF gene (Supplementary Table 5 and Supplementary Fig. 8). *BCL7A* was among the most frequently mutated SWI/SNF genes in DLBCL patients, together with *ARID1A, ARID1B, SMARCA4,* and *ACTB*. We found no significant co-occurrence or mutual exclusion of mutations between any pair of SWI/SNF subunits (Fisher's exact test, $P > 0.05$). Mutations in the SWI/SNF complex preferentially affected GCB-DLBCL samples when compared with ABC-DLBCLs (34.1–51.8% vs. 24.0–36.6% of mutant DLBCL patients) (Supplementary Table 5). Although this trend was observed for several SWI/SNF genes, it was only statistically significant for *BCL7A*, which was mutated in 8.8–13.4%

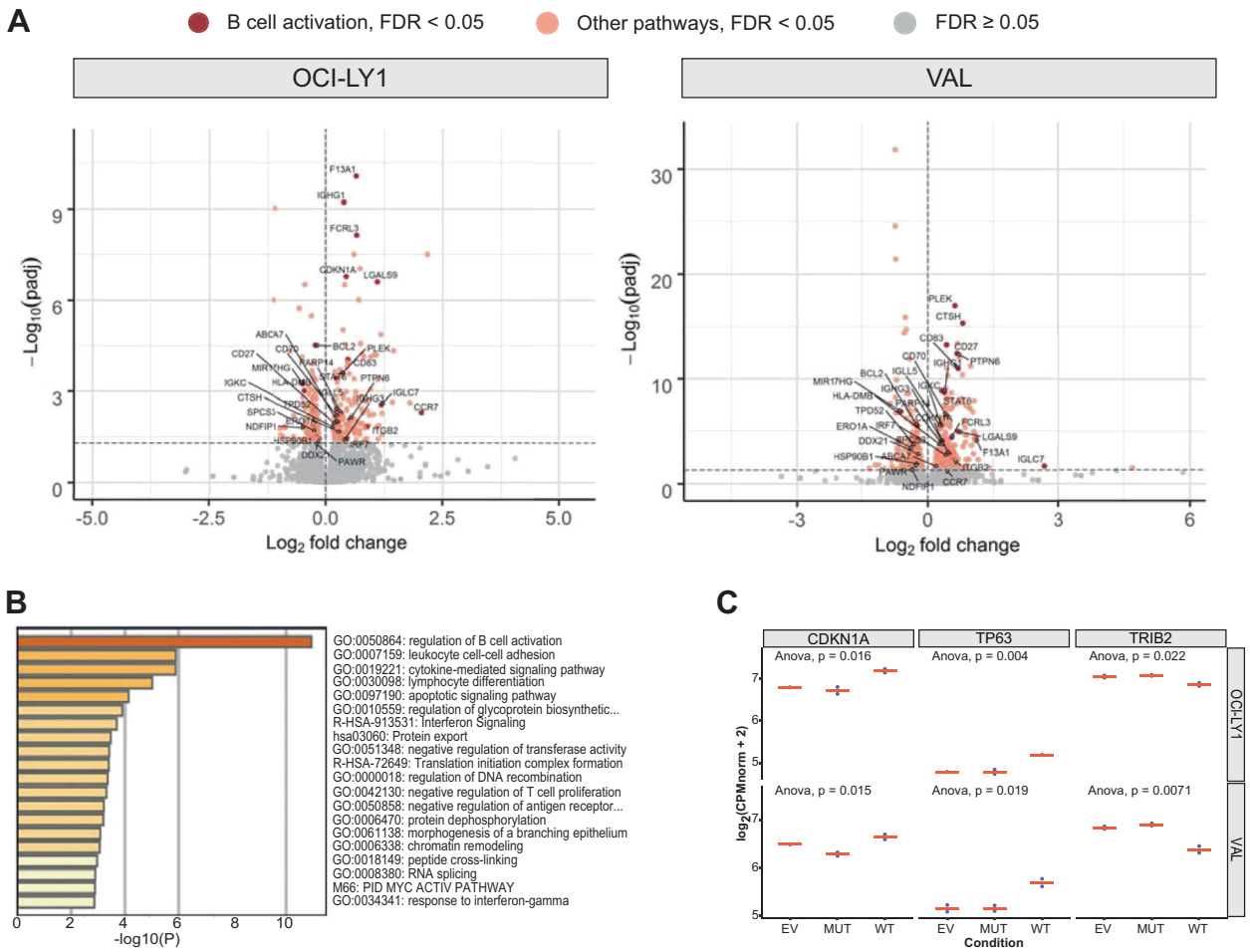

Fig. 5 RNA-seq differential expression analyses on the OCI-LY1 and VAL cell lines after overexpression of wild-type BCL7A vs. overexpression of Δ27-BCL7A. a Volcano plots highlighting the differentially expressed genes in OCI-LY1 (left) and VAL (right) cell lines. Genes belonging to the "regulation of B-cell activation" pathway family according to our GO enrichment analysis are shown in a darker red and their names are shown. **b** Enriched terms across the 162 differentially expressed genes found in common between OCI-LY1 and VAL. **c** Expression values according to our RNA-seq data of three selected genes: *CDKN1A*, *TP63*, and *TRIB2*. Gene expression counts normalized by DESeq2 were transformed to counts per million (CPMnorm) and log-transformed using cpm(…, log = TRUE, prior. count = 2) in R. The red horizontal lines represent the mean. ANOVA *p* values are shown.

GCB patients, 3.8–4.4% of ABC patients, and 5.3–6.1% of unclassified patients depending on the study. In addition, the top 50 most mutated genes in the dataset from Reddy et al. [25] were significantly enriched in chromatin remodeling functions and SWI/SNF genes, as we assessed by a GO analysis using enrichR [47] (Supplementary Table 6). Overall, our results point to a major role of the SWI/SNF chromatin remodeling complex in DLBCL, especially in GCB-DLBCL.

Discussion

Our study demonstrates for the first time that BCL7A plays a tumor suppressor role in DLBCL. BCL7A undergoes biallelic inactivation and, more importantly, it has a highly frequent mutational hotspot in the splice donor site of intron one. These mutations render a truncated BCL7A (Δ27-BCL7A) that is no longer able to bind to the SWI/SNF complex. Restoration of the expression of BCL7A, but not of Δ27-BCL7A, has a tumor suppressor-like phenotype both in vitro and in vivo. The tumor suppressor role of wild-type BCL7A and its functional differences with Δ27-BCL7A may be linked to a role of BCL7A in regulating the expression of genes related to B-cell activation processes, such as *CDKN1A*, *TP63*, and *TRIB2*.

BCL7A was first described when studying a three-way translocation involving *MYC, IGH* [48], and an unknown gene on chromosome 12q24.31 in the Burkitt lymphoma-derived Wien 133 cell line [49]. The authors named the unknown gene *BCL7A* using the acronym "BCL" (B-cell lymphoma) in the same way as other genes, such as *BCL2* and *BCL6*, that have been found to be involved in translocations in hematologic neoplasms [50]. However, BCL7A

has been less profusely studied than other "BCL" genes and its biological function remains largely unknown. Interestingly, the BCL7A/MYC/IGH three-way translocation resulted in the loss of the BCL7A amino-terminal region, which resembles the effect of the splice site mutations that we have characterized in our work.

The application of NGS to DLBCL tumors have served to unveil a huge heterogeneity at molecular and clinical levels [3–5, 16], but sample size limitations of pioneer studies prevented the discovery of mutations that could be pathogenically relevant. More recent sequencing studies, with larger sample sizes, showed that BCL7A is recurrently mutated in DLBCL [25, 26]. However, as we have addressed, the original articles excluded the most recurrent *BCL7A* mutations in the splice donor site. When we reanalyzed raw data from Reddy et al. [25] and Schmitz et al. [26] to include splice site alterations, we found an increase of *BCL7A* mutations by 27.4% and 17%, respectively. Germline information from most of these patients was unavailable, but we have provided external evidence from DLBCL samples and from healthy cohorts of over 100,000 individuals supporting that our newly identified splice site mutations are unlikely to affect the germline. Furthermore, we have shown that *BCL7A* recurrently suffers biallelic loss in DLBCL cell lines and patients, a characteristic pattern of tumor suppressor genes [51]. In addition, the high allele frequencies of the majority of BCL7A inactivating mutations suggest that these mutations may be early drivers [52], which make *BCL7A* an attractive target for future research on clinical applications.

Importantly, our study has brought to light that the splice site mutations are the most frequent *BCL7A* mutations in DLBCL and, in addition, we have proven that they have a functional impact. These mutations render a shorter BCL7A protein (Δ27-BCL7A) that is no longer able to bind to the SWI/SNF complex in agreement with the need of BCL7_Nt domain to associate to other SWI/SNF complex subunits [53]. Although we have focused on the functional consequences of *BCL7A* splice site mutations, mutations in R11 are likely to have an important impact on BCL7A function. These mutations often coexist with mutations that are known to inactivate *BCL7A* (splicing, start loss, stop gain, and frameshift), but they are never present in the same allele. These patterns, together with the fact that R11 is the only significant hotspot of missense mutations in *BCL7A*, suggest a putative driver role of R11 mutations. In future work, it may be of interest to assess whether and how R11 mutations affect BCL7A function.

Mutations in *BCL7A*, clustering within the conserved BCL7-Nt domain, have been attributed to SHM. *BCL7A* mutations in coding and noncoding regions are more frequent in the endemic subtype in comparison with sporadic and immunodeficiency-associated Burkitt lymphomas and these differences have been associated to a higher AID activity [54]. AID-mediated mutations in genes including *BCL7A* have been linked to transformation of FL to DLBCL [55]. AID footprint could also explain *BCL7A* mutations in post-GC B cell derived lymphomas such as multiple myeloma, where *BCL7A* mutations are mainly found in noncoding regions [56]. Therefore, aberrant SHM seems to be a source of *BCL7A* mutations in B-cell malignancies while other mechanism such as promoter hypermethylation have been described to inactivate *BCL7A* in cutaneous T-cell lymphomas [57]. Overall, ongoing SHM could explain why *BCL7A* mutations seem to be restricted to GC-derived B-cell lymphomas, unlike other SWI/SNF genes that are mutated in a wide spectrum of tumors [17]. However, as we have addressed, although splice site mutations of *BCL7A* fall within an AID motif, their high frequency suggests a further mechanism of positive selection to provide a growth advantage in tumoral cells. In addition, the rest of the mutational hotspots or inactivating mutations of *BCL7A* in our analyses did not overlap with AID motifs. Taken together, these observations suggest that SHM is not the only mechanism of *BCL7A* mutagenesis.

Mutations in genes that encode for histone and chromatin modifiers are consistently found in DLBCL and other GC-derived lymphomas [10, 58]. The chromatin epigenome and hence transcriptional deregulation seem to play important roles in lymphomagenesis. In this sense, maintenance of a transcriptional repression state has been found to suppress B-cell differentiation to plasma cell, allowing B-cell affinity maturation within the GC. BCL6 and EZH2, a subunit of PRC2 complex, cooperate to maintain the transcriptional repression [59] and block B-cell differentiation to plasma cells. However, constitutive expression of *BCL6* as well as gain-of-function mutations in *EZH2* derive in GC hyperplasia [60, 61]. Although data about SWI/SNF function in hematologic cancers is yet missing, recent research in solid tumors has shown that loss of SWI/SNF complex integrity impairs SWI/SNF binding to typical enhancers, particularly those required for differentiation [13, 62]. Furthermore, the SWI/SNF complex opposes the activity of PRC complexes by their direct eviction [63]. In the context of lymphomagenesis, dysfunctional SWI/SNF complex could damage the eviction of PRC complexes and impair the regulation of the expression of genes required for B-cell differentiation, therefore allowing a continuous and exacerbated repressive state dictated by PRC complexes to avoid terminal differentiation.

EZH2 gain-of-function mutations ($EZH2^{Y641}$) are a hallmark of GC-derived lymphomas including GCB-DLBCL [64]. Mutant EZH2 is not sufficient for B-cell transformation into DLBCL but $EZH2^{Y641}$ in combination with overexpression of the oncogenes Bcl2 or Myc leads to an accelerated lymphoma onset in mouse models [61, 65]. Similarly, SWI/SNF complex inactivation and $EZH2^{Y641}$ gain-of-function mutations could synergize to maintain the

B-cell program and limit plasma cell differentiation, leading to tumorigenesis. In fact, BCL7A and EZH2 mutations tend to coexist in GCB-DLBCL, and more precisely in the "EZB" subtype described by Schmitz et al. [26], characterized by *EZH2* mutations and *BCL2* translocations. Interestingly, we have seen that BCL7A mutations only overlap with $EZH2^{Y641}$ gain-of-function mutations, and not with any other EZH2 mutation in both external datasets analyzed in this study (Supplementary Table 7). SWI/SNF mutant cancers have been shown to depend on the activity of EZH2 and EZH2 inhibition is a promising therapeutic tool against SWI/SNF mutant tumors [66, 67]. In early 2020, the EZH2 inhibitor Tazemetostat was approved by the FDA to treat epithelioid sarcomas lacking SMARCB1 expression. Currently, there are ongoing clinical trials to treat relapsed Non-Hodgkin Lymphoma patients bearing gain-of-function mutations in *EZH2*, or loss-of-function mutations in *SMARCA4* or *SMARCB1* [68]. Given the mutational burden of other SWI/SNF subunits such as BCL7A in GC-derived lymphomas it would be interesting to include *BCL7A* mutant patients in future clinical trials testing EZH2 inhibitors.

Additional evidence supports the involvement of BCL7A in the GC. *BCL7A* expression levels are modulated through the GC reaction [6, 24] and BCL6 activity has been shown to regulate *BCL7A* expression levels [69]. The need of BCL7A and, therefore, of the SWI/SNF complex in gene expression regulation during the GC reaction is supported by our RNA-seq analysis showing that wild-type BCL7A expression restoration is involved in B-cell activity pathways including lymphocyte differentiation and adhesion. *CDKN1A*, which is silenced by EZH2 to enable GC formation [61], was upregulated after we restored BCL7A expression in two DLBCL cell line models. These results agree with an opposing role of the SWI/SNF complex to PRC2 complex activity.

To summarize, we report the first experimental evidence of the tumor suppressor role of BCL7A in DLBCL. BCL7A mutations cluster within its conserved amino-terminal domain and loss of this domain has a functional impact on the ability of BCL7A to bind to the SWI/SNF complex. BCL7A inactivation impairs the regulation of the expression of genes related with B-cell biology and could contribute to lymphomagenesis. Overall, these discoveries remark the relevance of BCL7A in DLBCL, especially in the GCB subtype, and reveals new prognostic and/or therapeutic opportunities for the treatment of DLBCL patients.

Data availability

RNA-seq data discussed in this publication is accessible through Gene Expression Omnibus under accession number GSE149277. The mass spectrometry proteomics data have been deposited to the ProteomeXchange Consortium via the PRIDE partner repository with the dataset identifier PXD014795. Data will be available immediately following publication, no end date. All other data and processing code are available from the corresponding author upon reasonable request.

Acknowledgements PPM laboratory is supported by the Deutsche José Carreras Leukämie-Stiftung, Becas Leonardo (BBVA Foundation), the Ministry of Economy of Spain (SAF2015-67919-R), Consejería de Salud de la Junta de Andalucía (PI-0245-2017), Proyectos de I + D + I en el marco del programa operative FEDER Andalucía 2014–2020 (B-CTS-126-UGR18, PIGE-0440-2019) and, Asociación Española Contra el Cáncer (AECC). PPM laboratory would like to special acknowledge to the *Heroes hasta la Médula* Association and to the *Aula de Investigación sobre la Leucemia infantil: Héroes contra la Leucemia*. JAM-C is supported by Instituto de Salud Carlos III FIS (PI19/00818) and CIBERONC (CB16/12/00489). AA is funded by the Ministry of Science, Innovation and Universities, Spain (FPU17/00067). JCA-P is supported by a Marie Curie Fellowship (MSCA-IF-EF-RI, #837897). CB-G acknowledges the PhD program in Biochemistry and Molecular Biology, University of Granada. The funding agencies had no role in study design, data collection and analysis, decision to publish, or preparation of the paper. The Genomic Variation in Diffuse Large B-Cell Lymphomas study was supported by the Intramural Research Program of the National Cancer Institute, National Institutes of Health, Department of Health and Human Services. A full list of acknowledgements can be found in the Supplementary Note of the original article [25]. The results published here are in part based upon data generated by the NCI's Clinical Trials Sequence Program and The Cancer Genome Atlas (managed by the NCI and NHGRI). The datasets have been accessed through the NIH database for Genotypes and Phenotypes (dbGaP). Information about TCGA can be found at http://cancergenome.nih.gov.

Author contributions PPM conceived the study, coordinated the scientific team, and allocated the funding for the project; CB-G and MIR generated most of the experimental data; PPM and CB-G designed experiments, analyzed data, and wrote the paper; AA performed bioinformatics analyses; AA, MC, JCA-P, and JAM-C reviewed the paper; AFA-P, VGdY, and ARR designed, performed, and analyzed AID mutational study; SS-H and FM provided lentiviral vector reagents and expertize; EF-V and JM performed LC–MS/MS and proteomic data analysis; and JAM-C provided lymphoma expertise and samples. All the authors contributed with suggestions after a critical reading of the draft and approve its submission for publication.

Compliance with ethical standards

Conflict of interest The authors declare that they have no conflict of interest.

Publisher's note Springer Nature remains neutral with regard to jurisdictional claims in published maps and institutional affiliations.

References

1. Coiffier B, Lepage E, Briere J, Herbrecht R, Tilly H, Bouabdallah R, et al. CHOP chemotherapy plus rituximab compared with CHOP alone in elderly patients with diffuse large-B-cell lymphoma. N Engl J Med. 2002;346:235–42.

2. Lohr JG, Stojanov P, Lawrence MS, Auclair D, Chapuy B, Sougnez C, et al. Discovery and prioritization of somatic mutations in diffuse large B-cell lymphoma (DLBCL) by whole-exome sequencing. Proc Natl Acad Sci USA. 2012;109:3879–84.
3. Pasqualucci L, Trifonov V, Fabbri G, Ma J, Rossi D, Chiarenza A, et al. Analysis of the coding genome of diffuse large B-cell lymphoma. Nat Genet. 2011;43:830–7.
4. Morin RD, Mungall K, Pleasance E, Mungall AJ, Goya R, Huff RD, et al. Mutational and structural analysis of diffuse large B-cell lymphoma using whole-genome sequencing. Blood. 2013;122:1256–65.
5. Zhang J, Grubor V, Love CL, Banerjee A, Richards KL, Mieczkowski PA, et al. Genetic heterogeneity of diffuse large B-cell lymphoma. Proc Natl Acad Sci USA. 2013;110:1398–403.
6. Alizadeh AA, Eisen MB, Davis RE, Ma C, Lossos IS, Rosenwald A, et al. Distinct types of diffuse large B-cell lymphoma identified by gene expression profiling. Nature. 2000;403:503–11.
7. Rosenwald A, Wright G, Leroy K, Yu X, Gaulard P, Gascoyne RD, et al. Molecular diagnosis of primary mediastinal B cell lymphoma identifies a clinically favorable subgroup of diffuse large B cell lymphoma related to Hodgkin lymphoma. J Exp Med. 2003;198:851–62.
8. Rosenwald A, Wright G, Chan WC, Connors JM, Campo E, Fisher RI, et al. The use of molecular profiling to predict survival after chemotherapy for diffuse large-B-cell lymphoma. N Engl J Med. 2002;346:1937–47.
9. Thieblemont C, Briere J, Mounier N, Voelker HU, Cuccuini W, Hirchaud E, et al. The germinal center/activated B-cell subclassification has a prognostic impact for response to salvage therapy in relapsed/refractory diffuse large B-cell lymphoma: a bio-CORAL study. J Clin Oncol. 2011;29:4079–87.
10. Lunning MA, Green MR. Mutation of chromatin modifiers; an emerging hallmark of germinal center B-cell lymphomas. Blood Cancer J. 2015;5:e361.
11. Kadoch C, Crabtree GR. Mammalian SWI/SNF chromatin remodeling complexes and cancer: mechanistic insights gained from human genomics. Sci Adv. 2015;1:e1500447.
12. Saha A, Wittmeyer J, Cairns BR. Chromatin remodelling: the industrial revolution of DNA around histones. Nat Rev Mol Cell Biol. 2006;7:437–47.
13. Wang X, Lee RS, Alver BH, Haswell JR, Wang S, Mieczkowski J, et al. SMARCB1-mediated SWI/SNF complex function is essential for enhancer regulation. Nat Genet. 2017;49:289–95.
14. Medina PP, Romero OA, Kohno T, Montuenga LM, Pio R, Yokota J, et al. Frequent BRG1/SMARCA4-inactivating mutations in human lung cancer cell lines. Hum Mutat. 2008;29:617–22.
15. Medina PP, Sanchez-Cespedes M. Involvement of the chromatin-remodeling factor BRG1/SMARCA4 in human cancer. Epigenetics. 2008;3:64–8.
16. Morin RD, Mendez-Lago M, Mungall AJ, Goya R, Mungall KL, Corbett RD, et al. Frequent mutation of histone-modifying genes in non-Hodgkin lymphoma. Nature. 2011;476:298–303.
17. Kadoch C, Hargreaves DC, Hodges C, Elias L, Ho L, Ranish J, et al. Proteomic and bioinformatic analysis of mammalian SWI/SNF complexes identifies extensive roles in human malignancy. Nat Genet. 2013;45:592–601.
18. Dunaief JL, Strober BE, Guha S, Khavari PA, Alin K, Luban J, et al. The retinoblastoma protein and BRG1 form a complex and cooperate to induce cell cycle arrest. Cell. 1994;79:119–30.
19. Roberts CW, Galusha SA, McMenamin ME, Fletcher CD, Orkin SH. Haploinsufficiency of Snf5 (integrase interactor 1) predisposes to malignant rhabdoid tumors in mice. Proc Natl Acad Sci USA. 2000;97:13796–800.
20. Wang X, Werneck MB, Wilson BG, Kim HJ, Kluk MJ, Thom CS, et al. TCR-dependent transformation of mature memory phenotype T cells in mice. J Clin Investig. 2011;121:3834–45.
21. Schiaffino-Ortega S, Balinas C, Cuadros M, Medina PP. SWI/SNF proteins as targets in cancer therapy. J Hematol Oncol. 2014;7:81.
22. Whitehouse I, Flaus A, Cairns BR, White MF, Workman JL, Owen-Hughes T. Nucleosome mobilization catalysed by the yeast SWI/SNF complex. Nature. 1999;400:784–7.
23. Kaeser MD, Aslanian A, Dong MQ, Yates JR 3rd, Emerson BM. BRD7, a novel PBAF-specific SWI/SNF subunit, is required for target gene activation and repression in embryonic stem cells. J Biol Chem. 2008;283:32254–63.
24. Ramos-Medina R, Montes-Moreno S, Maestre L, Canamero M, Rodriguez-Pinilla M, Martinez-Torrecuadrada J, et al. BCL7A protein expression in normal and malignant lymphoid tissues. Br J Haematol. 2013;160:106–9.
25. Reddy A, Zhang J, Davis NS, Moffitt AB, Love CL, Waldrop A, et al. Genetic and functional drivers of diffuse large B cell lymphoma. Cell. 2017;171:481–94 e15.
26. Schmitz R, Wright GW, Huang DW, Johnson CA, Phelan JD, Wang JQ, et al. Genetics and pathogenesis of diffuse large B-cell lymphoma. N Engl J Med. 2018;378:1396–407.
27. Krysiak K, Gomez F, White BS, Matlock M, Miller CA, Trani L, et al. Recurrent somatic mutations affecting B-cell receptor signaling pathway genes in follicular lymphoma. Blood. 2017;129:473–83.
28. Kato L, Begum NA, Burroughs AM, Doi T, Kawai J, Daub CO, et al. Nonimmunoglobulin target loci of activation-induced cytidine deaminase (AID) share unique features with immunoglobulin genes. Proc Natl Acad Sci USA. 2012;109:2479–84.
29. Khodabakhshi AH, Morin RD, Fejes AP, Mungall AJ, Mungall KL, Bolger-Munro M, et al. Recurrent targets of aberrant somatic hypermutation in lymphoma. Oncotarget. 2012;3:1308–19.
30. Grande BM, Gerhard DS, Jiang A, Griner NB, Abramson JS, Alexander TB, et al. Genome-wide discovery of somatic coding and noncoding mutations in pediatric endemic and sporadic Burkitt lymphoma. Blood. 2019;133:1313–24.
31. Muramatsu M, Kinoshita K, Fagarasan S, Yamada S, Shinkai Y, Honjo T. Class switch recombination and hypermutation require activation-induced cytidine deaminase (AID), a potential RNA editing enzyme. Cell. 2000;102:553–63.
32. Pasqualucci L, Neumeister P, Goossens T, Nanjangud G, Chaganti RS, Kuppers R, et al. Hypermutation of multiple proto-oncogenes in B-cell diffuse large-cell lymphomas. Nature. 2001;412:341–6.
33. Perez-Duran P, Belver L, de Yebenes VG, Delgado P, Pisano DG, Ramiro AR. UNG shapes the specificity of AID-induced somatic hypermutation. J Exp Med. 2012;209:1379–89.
34. Alvarez-Prado AF, Perez-Duran P, Perez-Garcia A, Benguria A, Torroja C, de Yebenes VG, et al. A broad atlas of somatic hypermutation allows prediction of activation-induced deaminase targets. J Exp Med. 2018;215:761–71.
35. Rada C, Di Noia JM, Neuberger MS. Mismatch recognition and uracil excision provide complementary paths to both Ig switching and the A/T-focused phase of somatic mutation. Mol Cell. 2004;16:163–71.
36. Methot SP, Di Noia JM. Molecular mechanisms of somatic hypermutation and class switch recombination. Adv Immunol. 2017;133:37–87.
37. Rogozin IB, Kolchanov NA. Somatic hypermutagenesis in immunoglobulin genes. II. Influence of neighbouring base sequences on mutagenesis. Biochim Biophys Acta. 1992;1171:11–8.
38. Jadayel DM, Osborne LR, Coignet LJ, Zani VJ, Tsui LC, Scherer SW, et al. The BCL7 gene family: deletion of BCL7B in Williams syndrome. Gene. 1998;224:35–44.
39. Zhou Y, Zhou B, Pache L, Chang M, Khodabakhshi AH, Tanaseichuk O, et al. Metascape provides a biologist-oriented resource for the analysis of systems-level datasets. Nat Commun. 2019;10:1523.

40. Phan RT, Saito M, Basso K, Niu H, Dalla-Favera R. BCL6 interacts with the transcription factor Miz-1 to suppress the cyclin-dependent kinase inhibitor p21 and cell cycle arrest in germinal center B cells. Nat Immunol. 2005;6:1054–60.
41. Velichutina I, Shaknovich R, Geng H, Johnson NA, Gascoyne RD, Melnick AM, et al. EZH2-mediated epigenetic silencing in germinal center B cells contributes to proliferation and lymphomagenesis. Blood. 2010;116:5247–55.
42. Chae YS, Kim H, Kim D, Lee H, Lee HO. Cell density-dependent acetylation of DeltaNp63alpha is associated with p53-dependent cell cycle arrest. FEBS Lett. 2012;586:1128–34.
43. Tan SH, Yam AW, Lawton LN, Wong RW, Young RA, Look AT, et al. TRIB2 reinforces the oncogenic transcriptional program controlled by the TAL1 complex in T-cell acute lymphoblastic leukemia. Leukemia. 2016;30:959–62.
44. Hou Z, Guo K, Sun X, Hu F, Chen Q, Luo X, et al. TRIB2 functions as novel oncogene in colorectal cancer by blocking cellular senescence through AP4/p21 signaling. Mol Cancer. 2018;17:172.
45. Hodges C, Kirkland JG, Crabtree GR. The many roles of BAF (mSWI/SNF) and PBAF complexes in cancer. Cold Spring Harb Perspect Med. 2016;6:a026930.
46. Michel BC, D'Avino AR, Cassel SH, Mashtalir N, McKenzie ZM, McBride MJ, et al. A non-canonical SWI/SNF complex is a synthetic lethal target in cancers driven by BAF complex perturbation. Nat Cell Biol. 2018;20:1410–20.
47. Kuleshov MV, Jones MR, Rouillard AD, Fernandez NF, Duan Q, Wang Z, et al. Enrichr: a comprehensive gene set enrichment analysis web server 2016 update. Nucleic Acids Res. 2016;44:W90–7.
48. Zani VJ, Asou N, Jadayel D, Heward JM, Shipley J, Nacheva E, et al. Molecular cloning of complex chromosomal translocation t(8;14;12)(q24.1;q32.3;q24.1) in a Burkitt lymphoma cell line defines a new gene (BCL7A) with homology to caldesmon. Blood 1996;87:3124–34.
49. Nacheva E, Fischer P, Karpas A, Sherrington P, Hayhoe FG, Manolov G, et al. Complex translocation t(8;12;14) in a cell line derived from a child with nonendemic Burkitt-type acute lymphoblastic leukemia. Cancer Genet Cytogenet. 1987;28:145–53.
50. Willis TG, Dyer MJ. The role of immunoglobulin translocations in the pathogenesis of B-cell malignancies. Blood. 2000;96:808–22.
51. Weinhold N, Ashby C, Rasche L, Chavan SS, Stein C, Stephens OW, et al. Clonal selection and double-hit events involving tumor suppressor genes underlie relapse in myeloma. Blood. 2016;128:1735–44.
52. Kumar S, Warrell J, Li S, McGillivray PD, Meyerson W, Salichos L, et al. Passenger mutations in 2500 cancer genomes: overall molecular functional impact and consequences. 2018:280446. https://www.biorxiv.org/content/10.1101/280446v1.full.
53. Mashtalir N, D'Avino AR, Michel BC, Luo J, Pan J, Otto JE, et al. Modular organization and assembly of SWI/SNF family chromatin remodeling complexes. Cell. 2018;175:1272–88 e20.
54. Panea RI, Love CL, Shingleton JR, Reddy A, Bailey JA, Moormann AM, et al. The whole-genome landscape of Burkitt lymphoma subtypes. Blood. 2019;134:1598–607.
55. Pasqualucci L, Khiabanian H, Fangazio M, Vasishtha M, Messina M, Holmes AB, et al. Genetics of follicular lymphoma transformation. Cell Rep. 2014;6:130–40.
56. Chapman MA, Lawrence MS, Keats JJ, Cibulskis K, Sougnez C, Schinzel AC, et al. Initial genome sequencing and analysis of multiple myeloma. Nature. 2011;471:467–72.
57. van Doorn R, Zoutman WH, Dijkman R, de Menezes RX, Commandeur S, Mulder AA, et al. Epigenetic profiling of cutaneous T-cell lymphoma: promoter hypermethylation of multiple tumor suppressor genes including BCL7a, PTPRG, and p73. J Clin Oncol. 2005;23:3886–96.
58. Pasqualucci L, Dalla-Favera R. Genetics of diffuse large B-cell lymphoma. Blood. 2018;131:2307–19.
59. Beguelin W, Teater M, Gearhart MD, Calvo Fernandez MT, Goldstein RL, Cardenas MG, et al. EZH2 and BCL6 cooperate to assemble CBX8-BCOR complex to repress bivalent promoters, mediate germinal center formation and lymphomagenesis. Cancer Cell. 2016;30:197–213.
60. Cattoretti G, Pasqualucci L, Ballon G, Tam W, Nandula SV, Shen Q, et al. Deregulated BCL6 expression recapitulates the pathogenesis of human diffuse large B cell lymphomas in mice. Cancer Cell. 2005;7:445–55.
61. Beguelin W, Popovic R, Teater M, Jiang Y, Bunting KL, Rosen M, et al. EZH2 is required for germinal center formation and somatic EZH2 mutations promote lymphoid transformation. Cancer Cell. 2013;23:677–92.
62. Mathur R, Alver BH, San Roman AK, Wilson BG, Wang X, Agoston AT, et al. ARID1A loss impairs enhancer-mediated gene regulation and drives colon cancer in mice. Nat Genet. 2017;49:296–302.
63. Kadoch C, Williams RT, Calarco JP, Miller EL, Weber CM, Braun SM, et al. Dynamics of BAF-Polycomb complex opposition on heterochromatin in normal and oncogenic states. Nat Genet. 2017;49:213–22.
64. Morin RD, Johnson NA, Severson TM, Mungall AJ, An J, Goya R, et al. Somatic mutations altering EZH2 (Tyr641) in follicular and diffuse large B-cell lymphomas of germinal-center origin. Nat Genet. 2010;42:181–5.
65. Berg T, Thoene S, Yap D, Wee T, Schoeler N, Rosten P, et al. A transgenic mouse model demonstrating the oncogenic role of mutations in the polycomb-group gene EZH2 in lymphomagenesis. Blood. 2014;123:3914–24.
66. Bitler BG, Aird KM, Garipov A, Li H, Amatangelo M, Kossenkov AV, et al. Synthetic lethality by targeting EZH2 methyltransferase activity in ARID1A-mutated cancers. Nat Med. 2015;21:231–8.
67. Kim KH, Kim W, Howard TP, Vazquez F, Tsherniak A, Wu JN, et al. SWI/SNF-mutant cancers depend on catalytic and non-catalytic activity of EZH2. Nat Med. 2015;21:1491–6.
68. Mittal P, Roberts CWM. The SWI/SNF complex in cancer—biology, biomarkers and therapy. Nat Rev Clin Oncol. 2020. https://doi.org/10.1038/s41571-020-0357-3.
69. Shaffer AL, Yu X, He Y, Boldrick J, Chan EP, Staudt LM. BCL-6 represses genes that function in lymphocyte differentiation, inflammation, and cell cycle control. Immunity. 2000;13:199–212.